Polymorphism of Crystalline α-Quaterthiophene and α-Sexithiophene: Ab Initio Analysis and Comparison with Inelastic Neutron Scattering Response

P. Hermet,* J.-L. Bantignies, A. Rahmani,† and J.-L. Sauvajol

Laboratoire des Colloïdes, Verres et Nanomatériaux (UMR CNRS 5587), Université Montpellier II, 34095 Montpellier Cédex 5, France

M. R. Johnson

Institut Laue-Langevin, B.P. 156, 38042 Grenoble Cédex 9, France

Received: February 15, 2005; In Final Form: March 16, 2005

Phonons in the α-quaterthiophene (4T) and α-sexithiophene (6T) polymorph phases are investigated using the direct method combined with density functional theory (DFT)-based total energy calculations. The simulation of inelastic neutron scattering spectra (INS) on the LT and HT polymorph phases of 4T and 6T enable the corresponding spectral signatures of these materials to be identified. In particular, there are two fingerprints: (i) the low-frequency vibrational modes (frequencies lower than 200 cm^{-1}) and (ii) the vibrational modes in the 600−900 cm^{-1} frequency range. The good agreement with the INS experimental data allows us to assign unambiguously the origin of all features (first-order and high-order processes) of these spectra and to predict that the LT phase is the phase measured experimentally both on the 4T and 6T materials. Moreover, the broad background in the 600−1400 cm^{-1} frequency range and the well-defined features which appear around 940 cm^{-1} in the calculated INS spectra of 4T/HT and 6T/HT are assigned to multiphonon contributions. This multiphonon contribution at 940 cm^{-1}, which is absent in the 4T/LT and 6T/LT INS spectra, also constitutes a fingerprint of the HT phases. Finally, the calculated dispersion curves of the two polymorph phases of 4T and 6T are given.

I. Introduction

Among the conjugated organic polymers, polythiophene has attracted considerable attention for technological applications because of its interesting electronic properties and its excellent chemical stability.[1−4] However, polythiophene presents a number of characteristics, such as low-crystallinity and chemical defects, that makes it difficult to establish a precise relationship between structure, vibrations, and electronic properties. In this context, oligothiophenes, with a perfectly controlled structure and a short chain length, have become important both as model compounds for polythiophene and as a novel class of molecular materials.[5] In these materials, the presence of long-range delocalization of π-conjugated systems on neighboring rings govern their optical and conducting/semiconducting properties.[6,7] Of particular interest are the phonons in the solid state of these systems because these modes can promote or hinder the $\pi-\pi^*$ overlap which is directly correlated to electronic transport.[8]

All unsubstituted oligothiophenes crystallize in the same monoclinic space group number 14 (e.g., $P2_1/a$, $P2_1/c$, or $P2_1/n$)[9] and pack in a herringbone structure. The number of molecules per unit cell may be either $Z = 2$ or 4. α-Bithiophene (2T) belongs to the first group,[10] whereas α-quaterthiophene (4T) and α-sexithiophene (6T) pertain to the second one.[11,12] However, 4T and 6T materials have been independently reported under both forms, depending on the technique of crystal growth: single crystals grown from the vapor phase (low temperature, LT) pack with $Z = 4$ (4T/LT[11] and 6T/LT[12]), whereas those grown from the melt (high temperature, HT) are characterized by $Z = 2$ (4T/HT[11,13] and 6T/HT[14]). So, polymorphism, which in this work relates to the ability of a molecule to adopt different crystal structures, is an important phenomenon for the study of structure, vibrations, and electronic relationships. Since polymorphic materials have different intermolecular geometries and different local electronic structures, vibrational spectroscopy experiments, and particularly inelastic neutron scattering (INS) experiments, are an ideal and sensitive probe of polymorphism and they can provide complementary structural information to that obtained from X-ray diffraction experiments for instance. In this context, we seek a clear understanding of the polymorphism of 4T and 6T materials from the assignments of their INS spectra in the crystalline phase.

The experimental phonon density-of-states (DOS) of 4T and 6T in their crystalline phase have been measured in the 20−4000 cm^{-1} frequency range by INS experiments at low-temperature.[15] No information on the polymorph phase of these materials is indicated in the corresponding publication. Ab initio simulations of the INS spectra of a 4T and 6T isolated molecule were performed by Degli Esposti et al.[15,16] and compared with the experimental INS data obtained respectively on a 4T and 6T crystalline phase sample. Good agreement was found between experimental and calculated frequencies for the intramolecular modes in the 300−1600 cm^{-1} frequency range. Nevertheless, because the intermolecular interactions were not taken into account in the calculations, the intensities of the experimental INS spectra were not accurately reproduced. Moreover, in the case of the isolated molecule, information about the polymorphism of 4T and 6T materials is not available. Consequently, there is no accurate theoretical or experimental assignment of the vibrational modes on the LT and HT

* Corresponding author. E-mail: hermet@lcvn.univ-montp2.fr.
† Permanent address: Département de Physique, Université MY Ismail, Faculté des Sciences, B. P. 4010, 50000 Meknès, Morocco.

10.1021/jp050798e CCC: $30.25
Published on Web 04/14/2005

polymorph phases of 4T and 6T in the literature, and there is no characteristic vibrational mode which allows the LT and HT polymorph phases of 4T and 6T to be identified.

In this work, a complete assignment of the INS spectra on the LT and HT polymorph phases of 4T and 6T is reported by first-principles calculations using density functional theory[17,18] (DFT) coupled to the direct method.[19] This approach allows intermolecular, long-range interactions to be investigated using the supercell method, and it has already been used by our group to analyze INS spectra calculations of 2T crystalline phase.[20] The characteristic vibrational modes which allow the identification on the LT and HT phases of 4T and 6T will be emphasized by a direct comparison between the calculated INS spectra and the experimental ones.

This paper is organized as follows. In section II, we describe the computational details of our first-principles calculations and we give the method for calculating the INS spectra on the LT and HT polymorph phases of 4T and 6T. Section III presents the results of our first-principles calculations. We compare our calculated structural geometry relaxation on the LT and HT polymorph phases of 4T and 6T with the experimental X-ray diffraction experiments. Calculated INS spectra, including the influence of the multiphonon contributions up to five phonon processes, are compared to INS experiments. The calculated dispersion curves on the polymorph phases of 4T and 6T are also given in this section. Section IV presents a detailled analysis on the polymorphism of 4T and 6T. The vibrational modes which play an important role in the identification of the two polymorph phases of 4T and 6T from a INS spectrum are discussed in detail. Finally, section V concludes the paper.

II. Computational Details

A. First-Principles Calculations. Calculations of the vibrations in the crystalline phase of 4T/LT, 4T/HT, 6T/LT, and 6T/HT materials were performed using the Vienna ab initio simulation package[21−23] (VASP). Exchange-correlation effects were handled within the generalized gradient approximation (GGA) as proposed by Perdew, Burke, and Ernzerhof[24] (PBE) model. The interactions between ions and electrons were described by the projector augmented wave (PAW) method[25,26] in the real space representation. All our calculations were performed with a plane-wave energy cutoff of 280 eV. For the optimization procedure of the structures, we have considered a $1 \times 2 \times 1$ supercell for both the 4T/HT and 6T/HT phases, whereas a $2 \times 1 \times 1$ supercell was used for the 4T/LT phase. Since the number of atoms in the unit cell of the 6T/LT is important (176 atoms) and the calculation time in DFT methods scales with the third power of the number of atoms, no supercell has been considered for this system. Only the atomic coordinates were optimized to prevent unphysical expansion of the supercells due to the lack of long-range dispersive interaction in DFT-based methods.[20] In practice, each supercell was optimized by using a fine integration grid until the maximum residual force on the atoms was less than 3×10^{-4} eV/Å. The Brillouin zone was sampled according to the Monkhorst-Pack scheme[27] by using a $2 \times 3 \times 4$ *k*-points grid for the 4T/HT and 6T/HT phases, whereas a $3 \times 4 \times 1$ and a $5 \times 4 \times 1$ *k*-points grid were used respectively for the 4T/LT and 6T/LT phases. Both energy cutoff for plane-waves and *k*-points sampling were sufficient for convergence of the calculated INS responses.

B. Inelastic Neutron Scattering Spectrum Modeling. The normal modes were calculated in the harmonic approximation by using the direct method.[19] From each optimized structure, each atom of the asymmetric unit was displaced with an optimal magnitude along the three Cartesian directions to calculate the Hellmann−Feynman (HF) forces on each atom. Positive and negative displacements were used to minimize numerical errors in the HF force calculations. In these conditions, since there is respectively a total of 30, 15, 44, and 22 atoms in the asymmetric unit of 4T/LT,[11] 4T/HT,[11] 6T/LT,[12] and 6T/HT,[14] we have generated respectively 180, 90, 264, and 132 distorted structures. The amplitude of atomic displacement is an important choice.[20] For displacements which are too small, the forces and numerical noise are of the same order of magnitude, whereas for large displacements, the linear response theory breaks down. We have found that a displacement magnitude of 0.05 Å is optimal for the 4T/HT and the 6T/LT, whereas displacement magnitudes of 0.03 and 0.06 Å are optimal for the 4T/LT and the 6T/HT materials, respectively. The HF forces on the atoms of the asymmetric unit in each supercell were obtained from a single-point energy calculation on each corresponding perturbed structure. Finally, for each polymorph phases, the HF forces were given as input to the PHONON program[28] which generates and diagonalizes the dynamical matrix for any point in reciprocal space using the symmetry of the crystal structure. The dynamical matrix, and thus the DOS, was calculated for 1500 wavevectors chosen at random. The dynamical structure factor was calculated from the DOS for a polycrystalline powder. Finally, the calculated spectra were convoluted with a Gaussian, with a full width at half-maximum (fwhm) fixed at 2% of the energy transfer (close to the instrument resolution of TFXA spectrometer[15]). The contribution of multiphonons, up to five-phonon processes, was evaluated in the INS spectrum calculations.

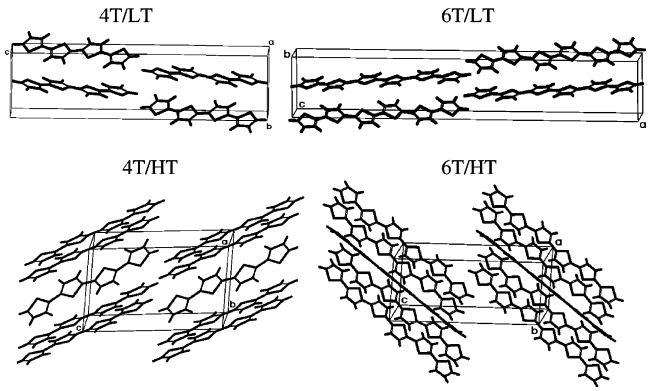

Figure 1. Single crystal on LT and HT polymorph phases of 4T and 6T with their axis reference systems.

In this work, since the identification of the calculated modes by comparison with experiment is unambiguous, we have not used a scale factor procedure to correct mode frequencies in our simulations.

III. Computational Results

A. Structure Relaxation. In its LT polymorph phase, the 4T (4T/LT) crystallizes in the monoclinic space group $P2_1/c$ with experimental values of the lattice constants of $a = 6.085$ Å, $b = 7.858$ Å, $c = 30.483$ Å, and $\beta = 91.81°$,[11] whereas the 6T (6T/LT) crystallizes in the monoclinic space group $P2_1/n$ with lattice constants of $a = 44.708$ Å, $b = 7.851$ Å, $c = 6.029$ Å, and $\beta = 90.76°$.[12] In its HT polymorph phase, the 4T (4T/HT) and the 6T (6T/HT) crystallize in the same monoclinic space group $P2_1/a$ with lattice constants of $a = 8.935$ Å, $b = 5.751$ Å, $c = 14.340$ Å, and $\beta = 97.22°$[11,13] and $a = 9.140$ Å, $b = 5.684$ Å, $c = 20.672$ Å, and $\beta = 97.78°$,[14] respectively (see Figure 1).

Table 1 summarizes the bond lengths obtained after the atomic relaxation on the LT and HT polymorph phases of 4T

TABLE 1: Optimized and Experimental Bond Lengths (in angstroms) on LT and HT Polymorph Phases of 4T and 6T[a]

	4T						6T					
	4T/LT			4T/HT			6T/LT			6T/HT		
	calc.	exp.	error	calc.	exp.	error	calc.	exp.	error	calc.	exp.	error
$C_{11}-C_{15}$							1.442	1.439	0.2	1.440	1.448	0.6
C_3-C_8	1.441	1.441	0.0	1.442	1.460	1.2	1.437	1.444	0.5	1.436	1.419	1.2
C_1-C_x	1.438	1.422	1.1	1.438	1.441	0.2	1.437	1.444	0.5	1.436	1.453	1.2
$C_{25}-C_{30}$	1.442	1.436	0.4				1.436	1.442	0.4			
$C_{33}-C_{37}$							1.440	1.441	0.1			
$C_{18}-C_{19}$							1.421	1.408	0.9	1.422	1.447	1.7
C_9-C_{10}	1.422	1.420	0.1	1.422	1.448	1.8	1.411	1.405	0.4	1.411	1.402	0.6
C_4-C_5	1.412	1.426	1.0	1.412	1.416	0.3	1.411	1.401	0.7	1.411	1.407	0.3
$C_{26}-C_{27}$	1.412	1.434	1.5				1.411	1.403	0.6			
$C_{31}-C_{32}$	1.420	1.430	0.7				1.411	1.405	0.4			
$C_{40}-C_{41}$							1.420	1.415	0.3			
$C_{17}-C_{18}$							1.382	1.342	3.0	1.382	1.364	1.3
$C_{15}-C_{19}$							1.391	1.388	0.2	1.393	1.409	1.1
$C_{10}-C_{11}$	1.382	1.314	5.2	1.382	1.332	3.7	1.392	1.365	2.0	1.393	1.357	2.6
C_8-C_9	1.391	1.386	0.4	1.393	1.386	0.5	1.394	1.363	2.3	1.394	1.374	1.5
C_3-C_4	1.392	1.389	0.2	1.393	1.367	1.9	1.394	1.370	1.7	1.394	1.372	1.6
C_1-C_5	1.394	1.334	4.5	1.393	1.352	3.0	1.394	1.379	1.1	1.395	1.365	2.2
$C_{23}-C_{27}$	1.394	1.350	3.2				1.394	1.367	2.0			
$C_{25}-C_{26}$	1.392	1.402	0.7				1.394	1.376	1.3			
$C_{30}-C_{31}$	1.391	1.393	0.1				1.394	1.369	1.8			
$C_{32}-C_{33}$	1.381	1.318	4.8				1.392	1.377	1.1			
$C_{37}-C_{41}$							1.391	1.402	0.8			
$C_{39}-C_{40}$							1.381	1.346	2.6			
$S_{16}-C_{17}$							1.716	1.709	0.4	1.716	1.708	0.5
$C_{15}-S_{16}$							1.739	1.730	0.5	1.734	1.720	0.8
$C_{11}-S_{12}$	1.717	1.743	1.5	1.715	1.700	0.9	1.740	1.737	0.2	1.736	1.737	0.1
C_8-S_{12}	1.737	1.713	1.4	1.738	1.736	0.1	1.741	1.737	0.2	1.738	1.744	0.3
S_2-C_3	1.737	1.714	1.3	1.739	1.728	0.6	1.740	1.731	0.5	1.738	1.742	0.2
C_1-S_2	1.741	1.756	0.8	1.740	1.730	0.6	1.741	1.735	0.3	1.738	1.718	1.2
$C_{23}-S_{24}$	1.740	1.748	0.4				1.741	1.733	0.5			
$S_{24}-C_{25}$	1.739	1.715	1.4				1.741	1.734	0.4			
$C_{30}-S_{34}$	1.740	1.717	1.3				1.741	1.736	0.3			
$C_{33}-S_{34}$	1.716	1.733	1.0				1.737	1.736	0.1			
$C_{37}-S_{38}$							1.737	1.722	0.9			
$S_{38}-C_{39}$							1.716	1.709	0.4			

[a] The errors are in percent. The *x* labels the atoms 23 or 1′ for the LT and HT polymorph phases, respectively.

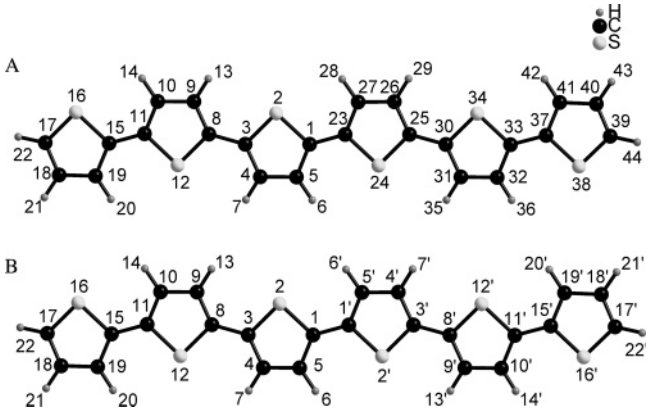

Figure 2. Molecule numbering scheme for the LT (A) and HT (B) polymorph phases. For the HT polymorph phase, primed atoms are related to unprimed ones by an inversion center at the midpoint of the $C_1-C_{1'}$ bond. Terminal carbon atoms in the molecules and those joined to the intercycle bonds are also called C_α atoms, whereas the other carbon atoms are called C_β atoms.

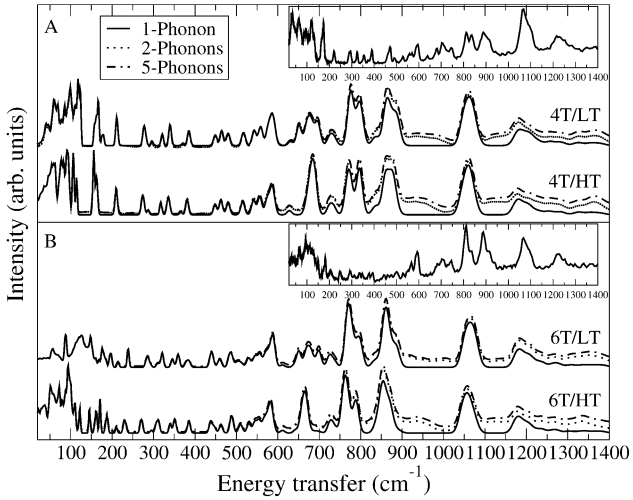

Figure 3. Calculated INS spectra on the LT and HT polymorph phases of 4T (A) and 6T (B) for one-, two-, and five-phonon contributions. Inset: experimental INS spectra of 4T and 6T from ref 15.

and 6T. Atom labels and numbering of 4T and 6T related to Table 1 are given in Figure 2. For both of the LT and HT polymorph phases, DFT calculations preserve the aromatic character of 4T and 6T. This is reflected by the $C_\beta-C_\beta$ calculated single bond which is longer than the $C_\alpha=C_\beta$ calculated double bonds in the thiophene rings. In agreement with X-ray diffraction experiments, DFT calculations pack the oligothiophene molecules as a herringbone structure and preserve the planar structure of the molecules. Generally, the optimized bond lengths are within 1−5% of the X-ray experimental values for both the LT and HT polymorph phases of 4T and 6T.

B. Multiphonon Effects. The broad contribution which appears in the 600−1400 cm^{-1} frequency range on the 4T and 6T experimental INS spectra is not clearly assigned in the

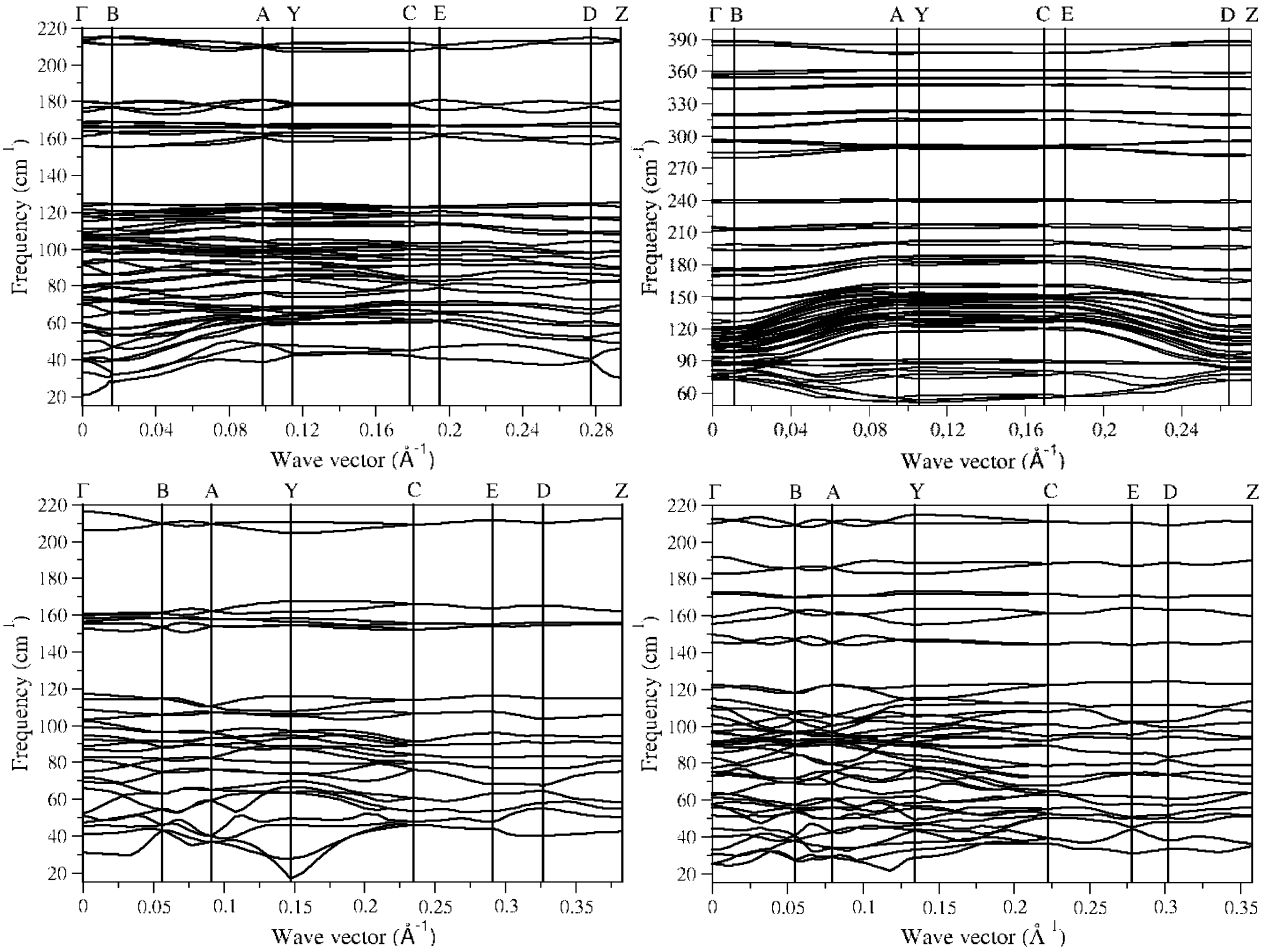

Figure 4. Calculated dispersion curves of LT (top) and HT (bottom) polymorph phases of 4T (left) and 6T (right). The labels denote the high-symmetry points in the Brillouin zone for the monoclinic system.

TABLE 2: Experimental and Calculated Frequencies (in cm^{-1}) of the 4T/LT and 4T/HT Phases with Their Assignments, Multiplicities, and Symmetries in the 600−920 cm^{-1} Frequency Range

	4T/LT				4T/HT			
exp.	calc.	mult.	symmetry	approximate assignments[a]	calc.	mult.	symmetry	approximate assignments[a]
639	630	1	B_g	δ(C$_\alpha$−S−C$_\alpha$)	627	1	A_g	δ(C$_\alpha$−S−C$_\alpha$)
680	654	2	$A_g + B_g$	γ(C−H) end of rings				
704	671	1	A_u	δ(C$_\alpha$−S−C$_\alpha$)	684	1	A_u	γ(C−H) end of rings
716	696	1	B_u	γ(C−H) end of rings				
746	727	4	$A_g + B_g + A_u + B_u$	δ(C$_\alpha$−S−C$_\alpha$)	726	1	B_u	δ(C$_\alpha$−S−C$_\alpha$)
813	776	1	A_u	γ(C−H) middle of rings	774	1	B_g	γ(C−H) middle of rings
835	795	1	A_g	γ(C−H) end of rings	795	1	B_u	γ(C−H) end of rings
875								
889	865	2	$B_g + B_u$	γ(C−H) middle of rings	864	1	A_g	γ(C−H)
917	888	3	$A_g + A_u + B_u$	γ(C−H) end of rings	879	1	A_g	γ(C−H) end of rings

[a] δ = in-plane bending, γ = out-of-plane bending.

literature (see inset Figure 3). The same profile appears on the experimental INS spectrum of 2T, and we have assigned this profile due to multiphonon contributions.[20] Because experiments have been performed at low temperature, only overtones and additive combination bands contribute to the INS spectra. In Figure 3, we show the calculated multiphonon contributions of higher order (from two to five) phonon scattering processes (i) to observe how the multiphonon processes alter the profile of the experimental INS spectra and (ii) to validate the fact that the multiphonon processes are responsible of the broad background which appears in the 600−1400 cm^{-1} frequency range of the experimental INS spectra. Figure 3 shows that the multiphonons contribute mainly to the background at higher frequency for both the LT and HT phases of 4T and 6T materials. In addition, in only the case of the HT structures, there is a reasonably well-defined feature at 940 cm^{-1} which is therefore assigned to a fingerprint of the HT phases.

C. Dispersion Curves. Monocrystals on different polymorph phases of 4T and 6T are not available, so full dispersion curves cannot be measured. On the basis of the good agreement between calculated and experimental INS spectra, the calculated dispersion curves, displayed in Figure 4, provide a reasonable picture of the real dispersion curves, except possibly for 6T/LT for which the simulation box has sides too small to simulate accurately the low frequencies. Indeed, the dispersion of the low frequency modes is only calculated correctly in larger supercells which allow all intermolecular interactions to be determined. This is the reason the dispersion curves of 6T/LT

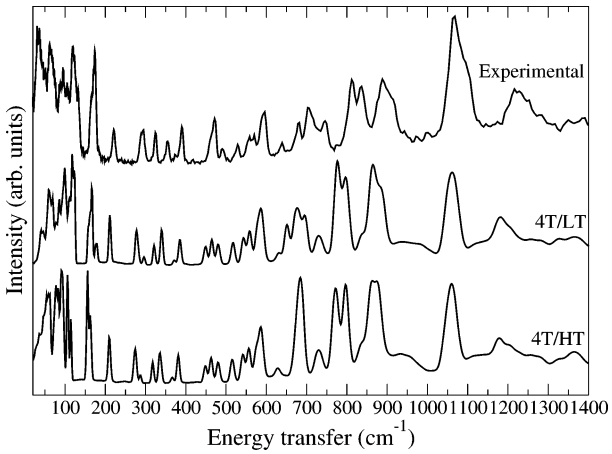

Figure 5. Comparison between the experimental and calculated INS spectra of 4T/LT and 4T/HT phases. The calculated spectra have been normalized on the experimental band centered at 593 cm^{-1}. Experimental spectrum from ref 15.

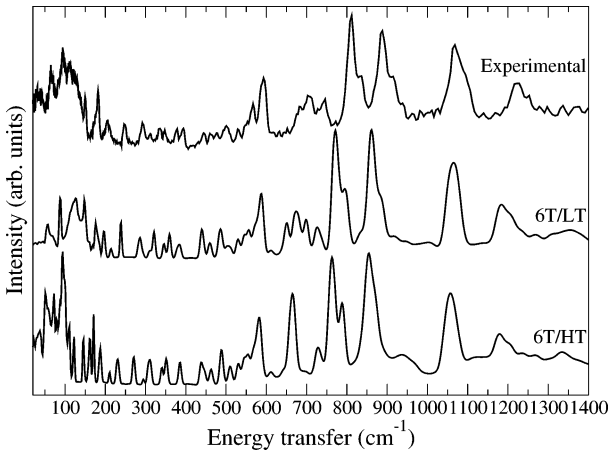

Figure 6. Comparison between the experimental and calculated INS spectra of 6T/LT and 6T/HT phases. The calculated spectra have been normalized on the experimental band centered at 593 cm^{-1}. Experimental spectrum from ref 15.

material start only from 60 cm^{-1}. The calculated dispersion curves of these materials are typical of covalent organic crystals. The optical branches do not show a large dispersion, thus giving rise to very sharp and narrow singularities in the vibrational DOS. Nevertheless, the fact that the optical branches are not flat showing a small, but nonnegligible dispersion, indicates that an intermolecular coupling between the different oligomers of the unit cell can occur. These calculated dispersion curves could be used to calculate all of the properties of the 4T and 6T crystalline phase in which phonon−phonon and electron−phonon interactions play an important role, as it is the case in electronic transport.

IV. Discussion

A. Identification of the Polymorph Phases of 4T. Figure 5 compares the experimental INS spectrum with the calculated ones on the LT and HT polymorph phases of 4T in the 20−1400 cm^{-1} frequency range. The complete assignments, frequencies, and symmetries of the calculated Γ-point normal modes on the LT and HT polymorph phases of 4T, in the 600−900 cm^{-1} frequency range, are given in Table 2. Among all points of the Brillouin zone, the Γ-point is of particular interest because only these modes can be infrared or Raman active. As the structure of the two polymorph phases of 4T and 6T are centrosymmetric (point group symmetry C_{2h}), the normal modes at the Γ-point are separated in infrared or Raman active modes. In Raman spectroscopy, only modes that transform under symmetry operations as a quadratic form (modes A_g and B_g) are active, whereas in infrared spectroscopy, only modes that transform as a vector (modes A_u and B_u) are active.

The direct comparison of the calculated spectra on the LT and HT polymorph phases with the experimental spectrum of 4T shows unambiguously than the LT phase is the phase measured experimentaly. Careful inspection of the external mode in the spectra (frequencies smaller than 200 cm^{-1}) shows better agreement for the 4T/LT structure with the experimental data. As the two polymorph phases are distinguished by the crystal packing of molecules in the unit cell, it is well-known that the low frequency vibrational modes are particularly sensitives to this effect. Concerning the high-frequency vibrational modes (frequencies higher than 200 cm^{-1}), it is, at first sight, surprising to observe that mainly intramolecular vibrational modes located in the 600−900 cm^{-1} frequency range are also a fingerprint of the polymorphic phases of 4T. Indeed, the experimental data and the 4T/LT calculated spectrum show a triplet of peaks centered at about 700 cm^{-1}, whereas the 4T/HT structure gives a single intense peak. An important difference between the LT and the HT structures of 4T materials is that the inversion center of the centrosymmetrical molecule does not coincide with a center of symmetry of the lattice in the LT structure, whereas it does in the HT structure. The displacements of the two halves of the molecule in 4T/HT modes present therefore symmetry about the center of the molecule, whereas this is not the case in the LT phase. In particular, this is the reason the C−H out-of-plane bending of the terminal thiophene rings gives a single mode calculated at 684 cm^{-1} for 4T/HT, whereas the corresponding modes are calculated at 654 and 696 cm^{-1} in 4T/LT due to the intermolecular interactions (see Table 2). So, these modes give rise to the multipeak structure in the 4T/LT spectrum at about 700 cm^{-1} which reproduces the experimental data.

B. Identification of the Polymorph Phases of 6T. In Figure 6, we report the calculated INS spectra on the LT and HT polymorph phases with the experimental spectrum of 6T in the 20−1400 cm^{-1} frequency range. The sensitivity of vibrational modes with respect to polymorphism is located in the same spectral region (600−900 cm^{-1} and frequencies lower than 200 cm^{-1}) to that discussed above for 4T and the assignments of vibrational modes are comparable. So, the comparison between the calculated LT and HT spectra with the experimental INS spectrum leads to the LT polymorph phase as being the phase measured experimentally.

Finally, it is interesting to note that the very intense band calculated around 670 cm^{-1} (see Figure 7), and assigned to a C−H out-of-plane bending of the terminal thiophene rings, can be considered as the fingerprint of a crystal packing of the HT polymorph phases associated to a unit cell with two molecules per unit cell in which the molecular inversion center is located at a crystallographic center of symmetry.

V. Conclusions

In conclusion, the INS spectra on the LT and HT polymorph phases of 4T and 6T, including multiphonon processes, have been calculated in a wide frequency range (20−1400 cm^{-1}) by first-principles calculations using DFT in combination with the direct method. The geometric parameters of the relaxed atomic structure of the two polymorph phases of 4T and 6T are found to be in good agreement with the experimental ones (at most 5% discrepancy). The most important result of this work is that

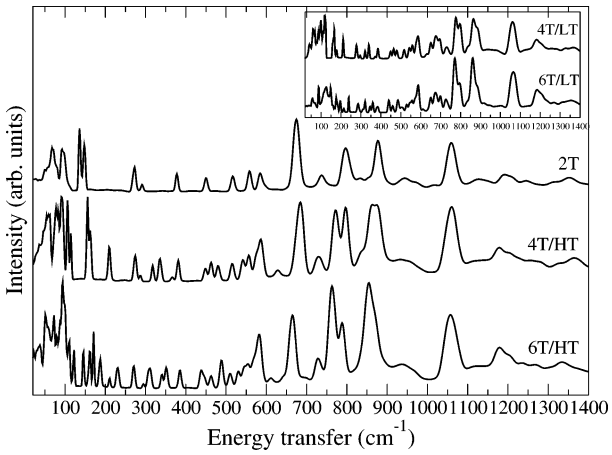

Figure 7. Calculated INS spectra of 2T, 4T/HT, and 6T/HT. Inset: calculated INS spectra of 4T/LT and 6T/LT. The calculated INS spectra have been normalized on the intense band centered around 670 cm^{-1}. Calculated INS spectrum of 2T is from ref 20.

the simulations of INS spectra enable the LT and HT polymorph phases of 4T and 6T to be distinguished. This identification is emphasized by two fingerprints: (i) the low-frequency external modes (frequencies lower than 200 cm^{-1}) and (ii) the vibrational modes in the 600−900 cm^{-1} frequency range. In this frequency range, we have calculated the phonons at the Γ-point of the Brillouin zone, given their assignment and symmetry. The good agreement with the experimental INS data allows us to assign unambiguously the origin of all features (first-order and high-order processes) of these spectra and to predict that the LT phase is the phase measured experimentally both on the 4T and 6T materials. We assign, both in the 4T and 6T materials, the broad background in the 600−1400 cm^{-1} frequency range and the reasonably well-defined features at around 940 cm^{-1} in the calculated INS spectra of 4T/HT and 6T/HT to multiphonon contributions. This multiphonon contribution at 940 cm^{-1}, which is absent in the 4T/LT and 6T/LT INS spectra, constitutes a fingerprint of the HT phases. In addition, these results demonstrate that the intense band around 670 cm^{-1} in the calculated INS spectra of 2T, 4T/HT, and 6T/HT can be considered as a signature of structure with two molecules per unit cell and a center of symmetry at the center of the molecule.

Finally, we emphasize that a coupled simulation/experiment approach can be generalized to study the polymorphism of materials from a direct comparison between the calculated vibrational spectra (in the DFT approach) and the experimental INS spectra. Recently, this work has been completed with success to the far- and mid-infrared simulations on the LT and HT polymorph phases of 4T in order to understand in more detail polymorphism on the experimental infrared spectra of this material.[29]

Acknowledgment. We are grateful to the CINES (Montpellier, France) for computational facilities on IBM SP3 computers.

References and Notes

(1) Roncali, J. *Chem. Rev.* **1992**, *92*, 711.
(2) Hotta, S.; Hosaka, T.; Shimotsuma, W. *Synth. Met.* **1983**, *6*, 69.
(3) Burroughes, J. H.; Bradley, D. D. C.; Brown, A. R.; Marks, R. N.; Mackay, K.; Friend, R. H.; Burn, P. L.; Holmes, A. B. *Nature* **1990**, *347*, 539.
(4) Tourillon, G.; Garnier, F. *J. Electrochem. Soc.* **1983**, *130*, 2042.
(5) Nalwa, H. S. *Handbook of Organic Conductive Molecules and Polymers*; Wiley: Chichester, U.K., 1997.
(6) Brédas, J. L.; Thémans, B.; André, J.; Chance, R.; Silbey, S. *Synth. Met.* **1984**, *9*, 265.
(7) Katz, H. E. *J. Mater. Chem.* **1990**, *7*, 369.
(8) Ginder, J. M.; Epstein, A. *J. Phys. Rev. B* **1990**, *41*, 10674.
(9) *International Tables of Crystallography*; Hahn, T., Ed.; Kluwer Academic Publishers: London, 1989.
(10) Pelletier, M.; Brisse, F. *Acta Crystallogr.* **1994**, *C50*, 1942.
(11) Siegrist, T.; Kloc, C.; Laudise, R. A.; Katz, H. E.; Haddon, R. C. *Adv. Mater.* **1998**, *10*, 379.
(12) Horowitz, G.; Bachet, B.; Yassar, A.; Lang, P.; Demanze, F.; Fave, J. L.; Garnier, F. *Chem. Mater.* **1995**, *7*, 1337.
(13) Antolini, L.; Horowitz, G.; Kouki, F.; Garnier, F. *Adv. Mater.* **1998**, *10*, 382.
(14) Siegrist, T.; Fleming, R. M.; Haddon, R. C.; Laudise, R. A.; Lovinger, A. J.; Katz, H. E.; Bridenbaugh, P.; Davis, D. D. *J. Mater. Res.* **1995**, *10*, 2170.
(15) Degli Esposti, A.; Moze, O.; Taliani, C.; Tomkinson, J. T.; Zamboni, R.; Zerbetto, F. *J. Chem. Phys.* **1996**, *104*, 9704.
(16) Degli Esposti, A.; Zerbetto, F. *J. Phys. Chem. A* **1997**, *101*, 7283.
(17) Hohenberg, P.; Kohn, W. *Phys. Rev.* **1964**, *136*, B864.
(18) Kohn, W.; Sham, L. J. *Phys. Rev.* **1965**, *140*, A1133.
(19) Parlinski, K. *Am. Inst. Phys. Conf. Proc.* **1999**, *479*, 121.
(20) Hermet, P.; Bantignies, J. L.; Rahmani, A.; Sauvajol, J. L.; Johnson, M. R. *J. Phys.: Condens. Matter* **2004**, *16*, 7385.
(21) Kresse, G.; Furthmüller, J. *Phys. Rev. B* **1996**, *54*, 11169.
(22) Kresse, G.; Furthmüller, J. *Comput. Math. Sci.* **1996**, *6*, 15.
(23) Kresse, G.; Hafner, J. *Phys. Rev. B* **1993**, *47*, 558.
(24) Perdew, J. P.; Burke, K.; Ernzerhof, M. *Phys. Rev. Lett.* **1996**, *77*, 3865.
(25) Kresse, G.; Joubert, D. *Phys. Rev. B* **1999**, *59*, 1758.
(26) Blöchl, P. E. *Phys. Rev. B* **1994**, *50*, 17953.
(27) Monkhorst, H. J.; Pack, J. D. *Phys. Rev. B* **1976**, *13*, 5188.
(28) Parlinski, K. Software PHONON, Cracow, 2001.
(29) Hermet, P.; Bantignies, J. L.; Sauvajol, J. L.; Johnson, M. R. manuscript submitted.